PNAS RESEARCH ARTICLE | NEUROSCIENCE OPEN ACCESS

Propofol-mediated loss of consciousness disrupts predictive routing and local field phase modulation of neural activity

Yihan (Sophy) Xiong[a], Jacob A. Donoghue[b], Mikael Lundqvist[b,c], Meredith Mahnke[b], Alex James Major[b], Emery N. Brown[b,d,e], Earl K. Miller[b,1], and André M. Bastos[a,f,1,2]

Affiliations are included on p. 11.

Edited by Stanislas Dehaene, College de France, Gif/Yvette, France; received September 6, 2023; accepted August 27, 2024

Predictive coding is a fundamental function of the cortex. The predictive routing model proposes a neurophysiological implementation for predictive coding. Predictions are fed back from the deep-layer cortex via alpha/beta (8 to 30 Hz) oscillations. They inhibit the gamma (40 to 100 Hz) and spiking that feed sensory inputs forward. Unpredicted inputs arrive in circuits unprepared by alpha/beta, resulting in enhanced gamma and spiking. To test the predictive routing model and its role in consciousness, we collected data from intracranial recordings of macaque monkeys during passive presentation of auditory oddballs before and after propofol-mediated loss of consciousness (LOC). In line with the predictive routing model, alpha/beta oscillations in the awake state served to inhibit the processing of predictable stimuli. Propofol-mediated LOC eliminated alpha/beta modulation by a predictable stimulus in the sensory cortex and alpha/beta coherence between sensory and frontal areas. As a result, oddball stimuli evoked enhanced gamma power, late period (>200 ms from stimulus onset) spiking, and superficial layer sinks in the sensory cortex. LOC also resulted in diminished decodability of pattern-level prediction error signals in the higher-order cortex. Therefore, the auditory cortex was in a disinhibited state during propofol-mediated LOC. However, despite these enhanced feedforward responses in the auditory cortex, there was a loss of differential spiking to oddballs in the higher-order cortex. This may be a consequence of a loss of within-area and interareal spike-field coupling in the alpha/beta and gamma frequency bands. These results provide strong constraints for current theories of consciousness.

predictive processing | oscillations | anesthesia | consciousness

Significance

Neurophysiology studies have found alpha/beta oscillations (8 to 30 Hz), gamma oscillations (40 to 100 Hz), and spiking activity during cognition. Alpha/beta power has an inverse relationship with gamma power/spiking. This suggests that gamma/spiking is under the inhibitory control of alpha/beta. The predictive routing model hypothesizes that alpha/beta oscillations selectively inhibit (to control) cortical activity that is predictable. We tested whether this inhibitory control is a signature of consciousness. We used multiarea neurophysiology recordings in monkeys presented with tone sequences that varied in predictability. We recorded brain activity as the anesthetic propofol was administered to manipulate consciousness. Compared to conscious processing, propofol-mediated loss-of-consciousness disrupted alpha/beta inhibitory control during predictive processing. This led to a disinhibition of gamma/spiking, consistent with the predictive routing model.

The idea that the brain makes inferences from environmental inputs has been generally accepted (1). Predictive coding is a prominent theoretical model of the inferential brain. It argues that previous experiences help construct an internal model which forms feedback predictions, and unexpected stimuli are fed forward, signaling prediction errors (2–4). Predictive coding is argued to be involved in cortical functions such as visual (5, 6) and auditory processing (7). Emerging cognitive paradigms and recording techniques have also revealed the potential involvement of predictive coding in higher-level cognition such as pattern recognition (8, 9).

The current paper tests a recent perspective, the predictive routing model, which implements predictive coding in the biological brain by mapping feedforward/feedback streams onto layer-specific brain rhythms and intrinsic anatomical connectivity (10). Predictions are fed back via deep-layer cortex alpha/beta (8 to 30 Hz) to prepare the cortex for receiving predicted input, and deviations from the predicted inputs (prediction errors) are fed forward via superficial-layer cortex gamma (40 to 100 Hz) and spiking (11–13). This model is supported by anatomical and neurophysiological findings. Anatomically, feedback neuronal connections originate in deep layers of the higher-order cortex and project onto superficial layers of the lower-order cortex (14, 15). Evidence from spike-field coherence indicates neurons in deep layers are alpha/beta coherent (16). Multi-laminar recordings across the cortex indicate that alpha/beta local field potential power is strongest in deep layers while gamma power is strongest in superficial layers (17, 18). Current sinks in both superficial and deep layers contribute to generating alpha/beta (13, 19, 20). This can be computationally modeled as alpha-rhythmic inputs to the superficial dendrites of deep-layer pyramidal neurons, indicating a potential role of L5 Martinotti cells (21).

An important theoretical extension from predictive coding to predictive routing is the role of oscillations in carrying out prediction and prediction error computations, instead of single neurons functioning as prediction error computation units. The predictive routing model specifically argues that feedforward gamma/spiking is inhibited by the alpha/beta feedback stream through the respective cortical layer-specific connections (10). The current

This article is a PNAS Direct Submission.

[1]E.K.M. and A.M.B. contributed equally to this work.

[2]To whom correspondence may be addressed. Email: andre.bastos@vanderbilt.edu.

This article contains supporting information online at https://www.pnas.org/lookup/suppl/doi:10.1073/pnas.2315160121/-/DCSupplemental.

Published October 7, 2024.

paper aims to causally test this model by measuring putative prediction error responses in the awake state, as well as anesthetized state using propofol, which profoundly decreases alpha/beta oscillations in posterior areas (22).

Propofol is a common anesthetic agent that enhances GABAergic activity, inducing loss of consciousness (LOC) (23). Under propofol-mediated LOC, the overall neuronal excitability, as measured by single neuron spike rate, is reduced across all cortical areas, and particularly strongly reduced in the lateral prefrontal cortex and frontal eye field than in the posterior auditory cortex (22). In addition, alpha/beta power is strongly reduced in the posterior cortex (parietal and visual cortex), as is cortico-cortical as well as cortico-thalamic alpha/beta phase coherence (22, 24). Previous work has linked interareal alpha/beta coherence to feedback influences (11–13). Here, we tested how this relatively greater decrease in frontal excitability (compared to sensory cortex excitability), together with a strong reduction in posterior alpha/beta power/coherence, would impact the processing of unexpected stimuli as a model of the predictive routing paradigm. We collected intracranial spike/LFP data in two macaque monkeys before and during propofol-mediated LOC while monkeys were presented with patterns of more or less predictable auditory stimuli. We hypothesized that since alpha/beta-dependent feedback is decreased during propofol-mediated LOC, that feedforward prediction error signals would become disinhibited (therefore increase in signal strength).

Two major models of consciousness have been under scientific discussion as of late: Global Neuronal Workspace theory (GNW) (25) and the Integrated Information Theory (IIT) (26). GNW posits that the subjective experience of consciousness emerges from communication in the prefrontal–parietal network, and that it is dependent on long-range broadcasting of information in this network. In contrast, IIT takes the approach of formalizing states of consciousness using a metric known as ϕ. It is calculated from binarized neural data (e.g., fMRI or neurophysiology data) and reflects the cause-effect structure present in the signal. From this formalism, proponents of IIT have theorized that a posterior "hot zone" is likely the more important substrate of conscious experience (27). In this account, neuronal activation of the hot zone is sufficient to induce conscious experience. Thus, the two theories diverge in their proposed network location of the neural correlates of consciousness, i.e., prefrontal–parietal in GNW and posterior hot zone in IIT. Empirical testing of these perspectives has been called upon (28) and the current study can inform this debate.

In this study, we provide two primary points of evidence to inform the GNW vs. IIT debate. First, we examine which areas (sensory vs. frontal) remain activated by an unpredicted stimulus during propofol-mediated LOC. Under the GNW theory, when subjects are unconscious, posterior areas may remain active but frontal areas will be inactive during processing of unpredictable stimuli. Under IIT, LOC will be primarily reflected in deactivation and/or discoordination of the posterior cortex. Second, we quantified the within- and interareal network coordination by calculating the strength of phasic coupling between alpha/beta and gamma LFP and spiking activity (similar to recent reports, e.g., ref. 29). Within-area, spike-LFP phasic modulation is thought to reflect the strength of functionally relevant local computations with increased coupling in gamma and decreased coupling in alpha/beta indexing enhanced computations (16, 30). Interareally, spike-LFP phasic modulation is thought to reflect the strength of interareal communication (31, 32). With respect to network coordination, GNW hypothesizes that LOC will primarily involve the loss of network coordination involving the frontal cortex. IIT on the other hand hypothesizes that a loss of network coordination within the posterior hot zone will primarily explain LOC.

In the current experiment, monkeys undergo a passive auditory oddball paradigm to elicit neuronal prediction and prediction error signals during propofol-mediated LOC. The auditory oddball paradigm has been used to generate prediction error signals in humans and nonhuman primates (8, 9, 33–35). A series of five pure tones is presented, with the first four always repeating (generating prediction), and the last tone having a different frequency (generating prediction error), which is referred to as local oddball (Fig. 1*A*). Some sequences are rare, known as global oddball trials, and these can be either local oddball trials (such as AAAAB trials in a block with the majority being AAAAA) or local regular trials (such as AAAAA trials in a block with the majority being AAAAB). Conversely, some sequences are frequent, and these are known as global regular trials. This passive auditory paradigm allows us to investigate neural coding differences both under awake state and following LOC when feedback alpha/beta is disrupted.

To investigate the hierarchical changes of predictive processing in the cortex, neural activity was recorded at various levels of the cortical hierarchy. This paper primarily focuses on the differential predictive effects in area Tpt (temporoparietal area, an auditory-responsive area in the superior temporal gyrus) and area FEF (frontal eye fields, a higher-order frontal area). To note, these two areas have been established to be anatomically connected (36). Hierarchical representation of prediction and prediction error has been proposed in the human cortex with data from noninvasive recording methods as well as intracranial recordings (37, 38). Thus, the current paper expands on this prior work by combining multiarea intracranial data from nonhuman primates including spiking, LFP, and cortical layer information, with a disruption of alpha/beta spike-LFP phasic modulation and consciousness via the anesthetic propofol (Fig. 1*B*).

Results

Characterizing Propofol-Mediated LOC. Using infusions of the anesthetic propofol, we induced LOC in two macaque monkeys over a period of 37 to 77 min in a total of eight independent sessions (Fig. 1*B*; see *Materials and Methods*). We confirmed LOC as behavioral nonresponsiveness and by the moment in which the eyelids spontaneously closed, similar to our recent report (22). We induced a cortical state characterized by increases in slow wave (~1 Hz) power, a reduction in alpha/beta and gamma power (*SI Appendix*, Fig. S1 *A* and *B*), and a reduction in spiking activity (from ~6 to 8 spikes per second during prepropofol awake baseline to ~1 spike per second during propofol-mediated LOC, *SI Appendix*, Fig. S1*C*). We refer to this cortical state as the anesthetized state or equivalently as propofol-mediated LOC. This level of anesthesia did not lead to burst suppression.

Loss of Local Oddball Spiking in the Frontal Cortex (FEF) but Not Sensory Cortex (Tpt) during Propofol-Mediated LOC. The predictive routing model hypothesizes that as stimuli become predictable (during regular trials, Fig. 1*A*), neural responses are inhibited by top–down beta rhythmic activity. Since spiking in the higher-order cortex is known to be more strongly reduced under propofol-mediated LOC compared to sensory areas, and because LOC is characterized by decreases in interareal alpha/beta synchronization (22), we hypothesized that spiking to oddballs in the higher-order cortex (FEF) will be more strongly reduced during propofol-mediated LOC than that in the lower-order cortex (Tpt).

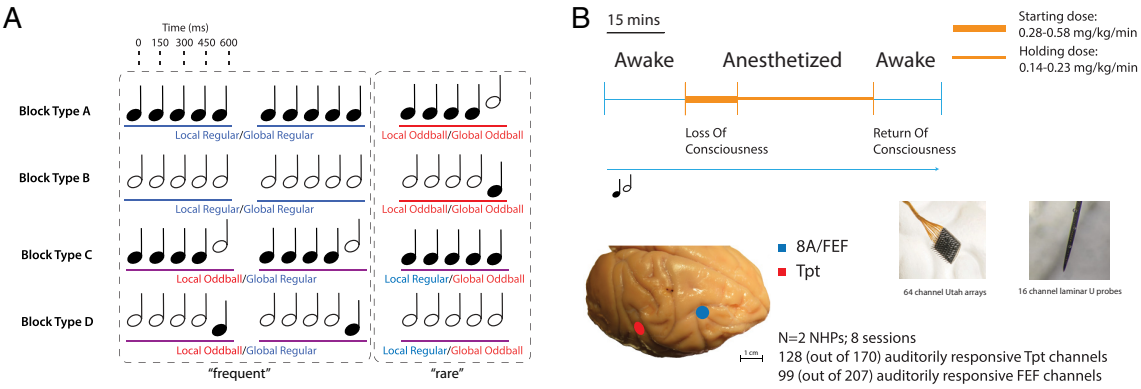

Fig. 1. Panel (*A*): Passive auditory oddball paradigm. Series of five tones are presented passively. Each block contains two types of patterns (AAAAA/BBBBB, "local regular trials" vs. AAAAB/BBBBA, "local oddball trials"). During each block, a pattern may be frequent ("global regular trials") or rare ("global oddball trials"). Panel (*B*): propofol infusion was initiated at a higher dose for ~20 min and maintained at a lower dose for ~40 min. Two types of probes were used (64-channel Utah arrays and 16-channel laminar U-probes). Neural data from areas Tpt and FEF were recorded.

To determine whether oddballs and regular trials in awake state and propofol-mediated LOC differed, ANOVA tests were performed at each time point (for every ms) to test for significant clusters in time of main effect of state (awake vs. LOC), main effect of condition (oddball vs. regular), and state by condition interactions.

Fig. 2*A* plots the MUA responses of FEF/Tpt for anesthetized and awake states, and separates local oddballs from local regulars (e.g., AAAAB vs. AAAAA, irrespective of whether these trials are rare vs. frequent). All ANOVA statistical tests reported in this section are based on testing time clusters of significance, corrected for multiple comparisons with a nonparametric cluster-based permutation test at $\alpha = 0.05$ (*Materials and Methods*). This revealed a main effect of local oddball condition in both area FEF and Tpt (Fig. 2*A*, purple bars, $p<0.05$). During propofol-mediated LOC, a differential (local oddball vs. local regular) response was preserved in area Tpt (Fig. 2 *A*, *Upper Right* subpanel). In contrast, the FEF response to local oddballs was largely eliminated during LOC (Fig. 2 *A*, *Lower Right* subpanel). This resulted in a significant state-by-oddball interaction in both areas Tpt and FEF, with an early (17 to 88 ms) reduction and late (158 to 383 ms) enhancement component in Tpt and only a reduction (~50 ms) component in FEF (Fig. 2*A*, blue bars).

The results also showed a main effect of state (awake vs. propofol-mediated LOC) in both areas (green bars in Fig. 2*A*). We further characterized the main effect of propofol in *SI Appendix*, Fig. S1*C*. This showed significant reductions in baseline as well as stimulus-driven spiking activity during propofol, replicating our recent report (22). In addition, single-unit spiking activity showed largely consistent oddball and state effects as compared to MUA activity (*SI Appendix*, Fig. S2). To summarize, propofol-mediated LOC *increased* the differential late (158 to 383 ms) local oddball vs. regular spiking responses in area Tpt and eliminated responses in FEF, while reducing overall spiking in both areas.

Higher-Order Cortex Coding of Global Oddballs Is Eliminated during Propofol-Mediated LOC. Fig. 2*B* plots the MUA responses of FEF/Tpt for anesthetized and awake states and separates all four mutually exclusive conditions (local oddball/global oddball, local oddball/global regular, local regular/global oddball, local regular/global regular). A main effect of global oddball status (i.e., rare vs. frequent, irrespective of AAAAB vs. AAAAA) was not found to be significant ($P > 0.05$). However, when examining the four mutually exclusive conditions (shown in Fig. 2*B*), condition-wise contrasts revealed significantly increased spiking during local oddball/global oddball trials compared to local oddball/global regular trials (Fig. 2*B* for MUA, purple bars indicate significance controlled for multiple comparisons; *SI Appendix*, Fig. S4 for single-unit analysis). We did not find that local regular/global oddball trials (blue MUA traces in Fig. 2*B*) differed from local regular/global regular trials (black traces in Fig. 2*B*) when correcting for multiple comparisons.

For each MUA channel in our sample, we defined the local effect as the rank sum statistic when comparing all local oddball trials to all local regular trials for 400 ms after fifth stimulus onset, and defined the global effect as the rank sum statistic when comparing all global oddball trials to all global regular trials for 400 ms after fifth stimulus onset. Local and global effects of auditory-responsive channels are shown in a scatter plot (Fig. 2*C*). We separately grouped channels based on awake responses that showed only local oddball effects, only global effects, both, or neither (Fig. 2*D*). In Tpt, all groupings reduced in significance, except that the channels that were not originally significant during the awake state became significant during the anesthetized state ($P < 0.05$, Wilcoxon's rank sum test, Fig. 2 *D*, *Upper* subpanels). In contrast, all groupings reduced in significance in FEF during the anesthetized state ($P < 0.05$, Wilcoxon's rank sum test, Fig. 2 *D*, *Lower* subpanels). This suggests a disinhibition of predictive processing effects in the lower-order cortex but not higher-order cortex.

To further investigate the encoding of global oddball status, as it was absent from the spiking main effect (all global oddball trials compared to all global regular trials were not significantly different in terms of mean firing rates when correcting for multiple comparisons), we trained a multivariate decoder (*Materials and Methods*) to predict stimulus identity, local oddball status, and global oddball status (defining global oddball status as all frequent vs. all rare stimuli). Note that we included area PFC in this decoding analysis, as the prior literature suggests that while PFC lacks the auditory responsiveness from our selection criteria for other analyses, predictive information may still be encoded in population information (39). We found that the decoder performed significantly above chance for stimulus information and local oddball status (both during the awake state and anesthetized state), and that global oddball decoding performance was above chance in FEF and PFC but not in Tpt (*SI Appendix*, Fig. S5*A*). Further, global oddball decoding in the frontal cortex fell to chance during propofol-mediated LOC. This finding again corroborates the hypothesis that frontal cortex activity is particularly diminished under anesthesia, especially during complex predictive processing such as during global oddballs. Another decoder was trained to investigate the decodability of local regular/global oddball (e.g., AAAAA rare) trials from local regular/global regular trials (e.g., AAAAA frequent) trials. This

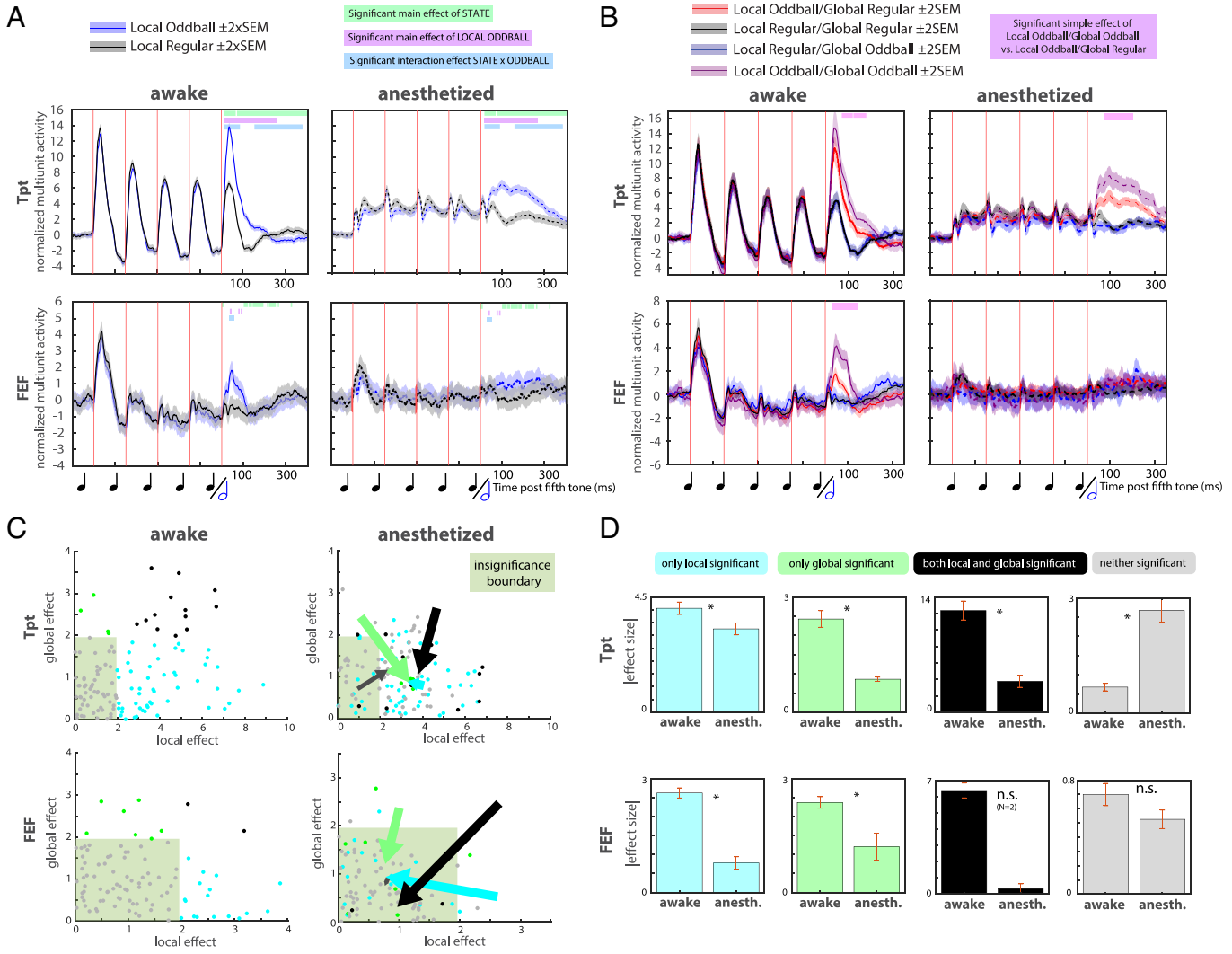

Fig. 2. Panel (*A*): Normalized and baselined multi-unit activity during a five-tone trial (shading represents ±2*SEM between trials). Red vertical lines show times of tone onset. Horizontal color bars post fifth tone show time clusters of significance (α = 0.05): purple for time periods of significant main effects of local oddball (considering both awake and anesthetized trials); blue for significant main effects of state (awake vs. anesthesia), and blue for significant interactions between state and oddball. Significance was tested using cluster-based permutation statistics, corrected for multiple comparisons (see *Materials and Methods*. N = 128 auditory-responsive Tpt channels, N = 99 auditory-responsive FEF channels. Panel (*B*): Normalized and baselined multi-unit activity during a five-tone trial (shading represents ±2*SEM between trials). Four mutually exclusive conditions are shown: 1) local regular/global regular (AAAAA frequent) 2) local oddball/global regular (AAAAB frequent) 3) local regular/global oddball (AAAAA rare) and 4) local oddball/global oddball (AAAAB rare). Red vertical lines show times of tone onset. N = 128 auditory-responsive Tpt channels, N = 99 auditory-responsive FEF channels. Horizontal green bars post fifth tone show time clusters of significant difference ($P < 0.05$) between local oddball/global regular and local oddball/global oddball conditions. Panel (*C*): *Left* subpanel: individual channel response effect sizes for local (AAAAB vs. AAAAA) and global (rare vs. frequent) contrasts under awake state. *Right* subpanel: individual channel response effect size (absolute values of the rank sum statistics comparing 400 ms after fifth stimulus onset) for local and global contrasts under anesthesia, and arrows representing the mean vector changes from awake to anesthetized, separately for channels that in the awake state are 1. Significant for the local contrast but not global contrast, 2. Significant for the global contrast but not local contrast, 3. Significant for both local and global contrasts, and 4. Significant for neither local nor global contrasts. Panel (*D*): mean absolute values of rank sum statistics for channels with the same groupings as in panel (*C*), comparing the awake state and anesthesia. For channels that were significant for either local or global effects, the bars show the respective previously significant rank sum statistics. For channels that were significant for both or neither, the bars show local effect rank sum statistics multiplied by global effect rank sum statistics.

comparison is often referred to in the literature as "pure" global oddballs, as the stimulus remains locally identical, and only the frequency of the sequence is compared. The decoder did not perform above chance ($P > 0.05$, *SI Appendix*, Fig. S5*B*).

As FEF is sensitive to eye movements, we performed an additional control analysis to rule out the contributions of eye movements to our results. Eye position and pupil size did not differ significantly during oddball vs. regular trials (*SI Appendix*, Fig. S6*A*). In addition, the local oddball effects were the same during trials in which the eyes were mostly open compared to trials in which the eyes were mostly closed (*SI Appendix*, Fig. S6*B*). Therefore, we conclude that the observed oddball effects above are not driven by eye movements or the open vs. closed state of the eyes.

In sum, these results showed that for local oddball compared to local regular, in Tpt the late spiking increase to local oddball emerged during propofol-mediated LOC compared to the awake state. In comparison, local oddball responses in FEF were entirely lost during propofol-mediated LOC compared to the awake state. In the case of global oddballs, while the main effect was not significant when considering all trials, our finding of enhanced spiking to rare vs. frequent local oddballs suggests that a prediction error is sent forward allowing the computation for a global prediction error as well (which is also encoded in population-level activity). This together suggests that top–down feedback is lost during LOC, leading to disinhibition of bottom–up inputs.

Since the strongest oddball effects were present in the comparison of all local oddball trials (local oddball/global oddball, local

oddball/global regular) to all local regular trials (local regular/global regular, local regular/global oddball), we restricted our further analyses in the rest of the manuscript to these trials to boost statistical power.

Disinhibition of Feedforward Gamma and Elimination of Feedback Alpha/Beta Modulation during Local Oddball Processing. It has been established that unpredictable stimuli evoke an increase in gamma-frequency power and a decrease in alpha/beta low frequency power in both sensory and higher-order cortex (9, 10, 37, 40, 41). Previous work has also shown a strong reduction in Tpt alpha/beta power and a reduction in fronto-parietal alpha/beta phase coherence during propofol (22, 24). In predictive routing, alpha/beta oscillations inhibit gamma. Therefore, we hypothesized that during propofol-mediated LOC, the cortex would be in an uninhibited state following an oddball stimulus.

To test this, we first compared LFP power in the awake state during local oddball trials vs. local regular trials. Out of a total of 207 channels recorded in FEF and 170 channels recorded in Tpt, we limited our analysis to 99 auditory-responsive channels in FEF and 128 auditory-responsive channels in Tpt (*Materials and Methods*). Consistent with predictive routing, both area Tpt and FEF showed increased gamma-frequency (>60 Hz) power following a local oddball, and increased alpha/beta frequency (15 to 30 Hz) power following a local regular (Fig. 3 *A* and *B, Upper* subpanels). We then compared local oddball vs. local regular trial LFP power during LOC. Gamma power increased in both area Tpt and FEF during local oddball (Fig. 3 *A* and *B, Lower* subpanels). In area Tpt, the gamma power percent increase to local oddball during LOC was higher than the awake state, suggesting disinhibition of the feedforward stream. The center frequency of the gamma power peak during 200 ms after local oddball onset lowered from 82 Hz during awake state to 40 Hz during LOC. Notably, alpha/beta decrease to local oddballs was lost during LOC in both areas ($P < 0.05$, Fig. 3*C*).

To further characterize alpha/beta power modulation during local oddball and local regular trials, we compared the power during sensory processing of oddballs/regulars to two different baselines to control for spontaneously occurring beta activity reported in previous work (42): immediately before fifth stimulus onset, and before the onset of the first tone. In both awake Tpt and FEF, alpha/beta power was highest during the pretrial baseline, lower during stimulus processing of regular trials, and was lowest during stimulus processing of oddball trials ($P < 0.05$, Wilcoxon's rank sum test, *SI Appendix*, Fig. S7). Under propofol-mediated LOC, alpha/beta power during stimulation compared to baseline was variable and evoked more subtle changes. Interestingly, the effect of oddball status reversed in its relationship with beta under anesthesia. Beta power significantly increased during oddballs as compared to regular trials in both Tpt and FEF $P < 0.05$, Wilcoxon's rank sum test, *SI Appendix*, Fig. S7).

These results are consistent with the hypothesized inhibitory top–down feedback role of alpha/beta in predictive routing, which becomes diminished under propofol-mediated LOC, leading to disinhibition of incoming sensory feedforward gamma from lower cortical areas.

Emergence of Stronger Current Sinks in Superficial Layers during Local Oddballs during Propofol-Mediated LOC Suggests Disinhibition of Feedforward Processing in the Microcircuit. Current source density analysis takes the second spatial derivative of the LFP and provides an estimate of laminar current flow in time (43). Middle layer inputs (i.e., current sinks in layer 4) are related to feedforward signals from lower-order areas, and superficial-layer (layers 2/3) sinks denote feedforward processes that will be sent to higher-order areas (2, 44). Current sinks were stronger in the middle layer (Fig. 4*C*) during local oddball compared to regular trials in area Tpt in the awake state ($P < 0.05$, corrected for multiple comparison with a nonparametric cluster-based permutation test at $\alpha = 0.05$, Fig. 4 *A–C*, note enhanced sink at times 0 to 200 ms post oddball onset). During LOC, this middle layer sink to local oddball was eliminated (Fig. 4*D*). Instead, a weaker superficial-layer sink emerged (Fig. 4*F*) and was stronger during local oddball than during local regular trials ($P < 0.05$, corrected for multiple comparison with a nonparametric cluster-based permutation test at $\alpha = 0.05$, Fig. 4 *D–F*). ANOVA on the time-space domain (corrected for multiple comparison with a nonparametric cluster-based permutation test at $\alpha = 0.05$; see *Materials and Methods*) confirmed the statistical significance of the state by condition interaction (Fig. 4*G*), such that the superficial-layer source to local oddball inversed into a sink during LOC (Fig. 4*H*). The emergence of a stronger sink in superficial layers further corroborates with previous evidence in LFP/MUA that the feedforward stream becomes disinhibited during unconscious processing of local oddballs. We also examined the potential layer differences in local oddball modulation. We show the oddball minus regular difference in single-unit spiking for superficial, middle, and deep-layer cells in *SI Appendix*, Fig. S8. In contrast to the CSD results, we do not observe any significant laminar effects, likely due to low sample size.

LFP Phase—MUA Coupling Patterns Suggested Disruption in Connectivity Following LOC. Slow wave (~1 Hz) spike-phase coupling is enhanced under propofol-mediated LOC (22), which was argued to result in the disruption of spike-phase coupling in faster frequencies such as alpha/beta and gamma (24). Since spike-phase coupling in alpha/beta and gamma is considered a mechanism of cortical communication (16, 24, 31, 45), the disruption of alpha/beta and gamma synchrony is hypothesized to be a mechanism of anesthesia-mediated LOC. So far, we have demonstrated that during propofol-mediated LOC, local oddball responses in the sensory cortex are disinhibited relative to the awake state. This was evidenced in area Tpt by a marked increase in gamma power to local oddballs, enhanced late (158 to 383 ms) spiking response to local oddballs, and enhanced superficial-layer CSD sink to local oddballs. At the same time, spiking and power responses in FEF to local oddballs are either diminished or eliminated during propofol-mediated LOC (Figs. 2 and 3). This begets the question of whether the eliminated FEF responses are due to disruptions in cortical communication either within- or interareas (or both).

To quantify neuronal communication, we used a metric of spike-phase coupling to quantify spike-LFP phasic modulation (*Materials and Methods*). With this method, the phase of an oscillation is used to fit MUA activity using a sinusoidal basis function. The R^2 of the fit reveals whether there is a relationship between phase and spiking. The amplitude of the resulting fit is a metric for how powerfully spiking activity is modulated by phase. The LFP phase at which the MUA activity peaks reflects coordination within and across areas, as these interactions may depend on an "optimal" phase (46, 47). We performed these fits as a function of area, frequency, and conscious state. For within-area spike-LFP phasic modulation, sinusoidal functions were fitted to the MUA on each channel as a function of local LFP alpha/beta and gamma phase (mean awake alpha/beta band fit $r^2 = 0.76$ in Tpt, $r^2 = 0.77$ in FEF; mean awake gamma band fit $r^2 = 0.79$ in Tpt, $r^2 = 0.75$ in FEF). In alpha/beta band phase to MUA pairs (N = 128 auditory-responsive Tpt channels, N = 99 auditory-responsive

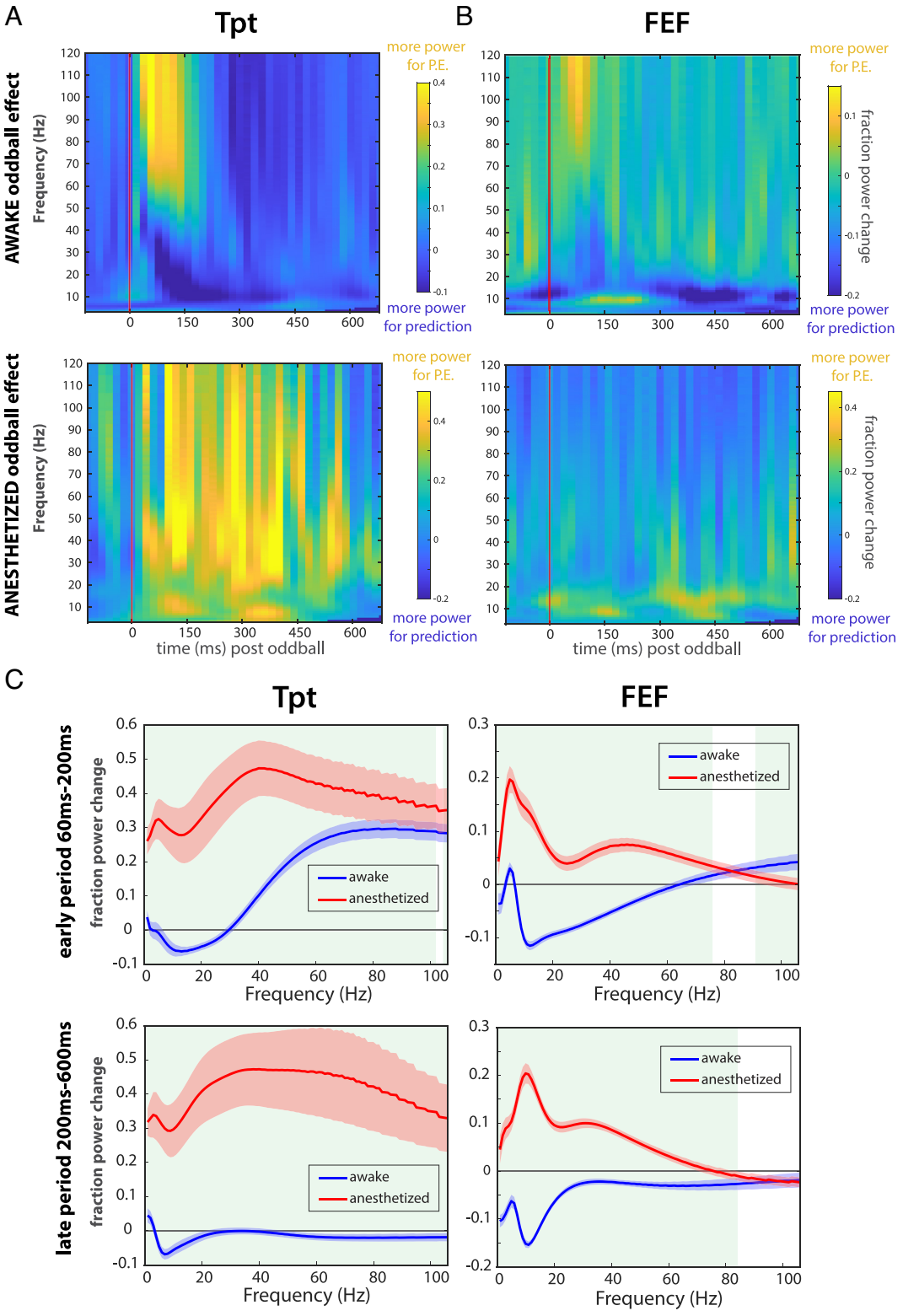

Fig. 3. Panels (*A* and *B*): Fraction power change from local regular to local oddball trials. Warmer color represents higher power in oddball trials, and cooler color represents higher power in regular trials. Panel (*A*) shows results from awake state and Panel (*B*) shows results from during LOC. Panel (*C*): Fraction power change (local oddball > local regular) by frequency for early vs. late period. Shading shows 2*SEM. Green blocks represent time periods during which the awake vs. propofol power change is significantly different.

FEF channels) the average amplitude of such fits was significantly decreased during LOC (Fig. 5, *Upper* subpanels, mean awake A = 0.0176 in Tpt, mean A = 0.0081 in FEF; mean propofol A = 0.0055 in Tpt, mean A = 0.0043 in FEF; mean per channel percent decrease in Tpt = 65.6%, mean per channel percent decrease in FEF = 28.6%; rank sum test, $P < 0.001$), suggesting that the strength of alpha/beta-spiking coupling was significantly weaker during LOC. Gamma band oscillations followed a similar pattern in terms of local modulation of MUA. Propofol-mediated LOC significantly decreased the amplitude of the sinusoidal fits on local MUA as a function of LFP (Fig. 5, *Upper* subpanels, mean awake A = 0.0220 in Tpt, mean A = 0.0105 in FEF; mean propofol

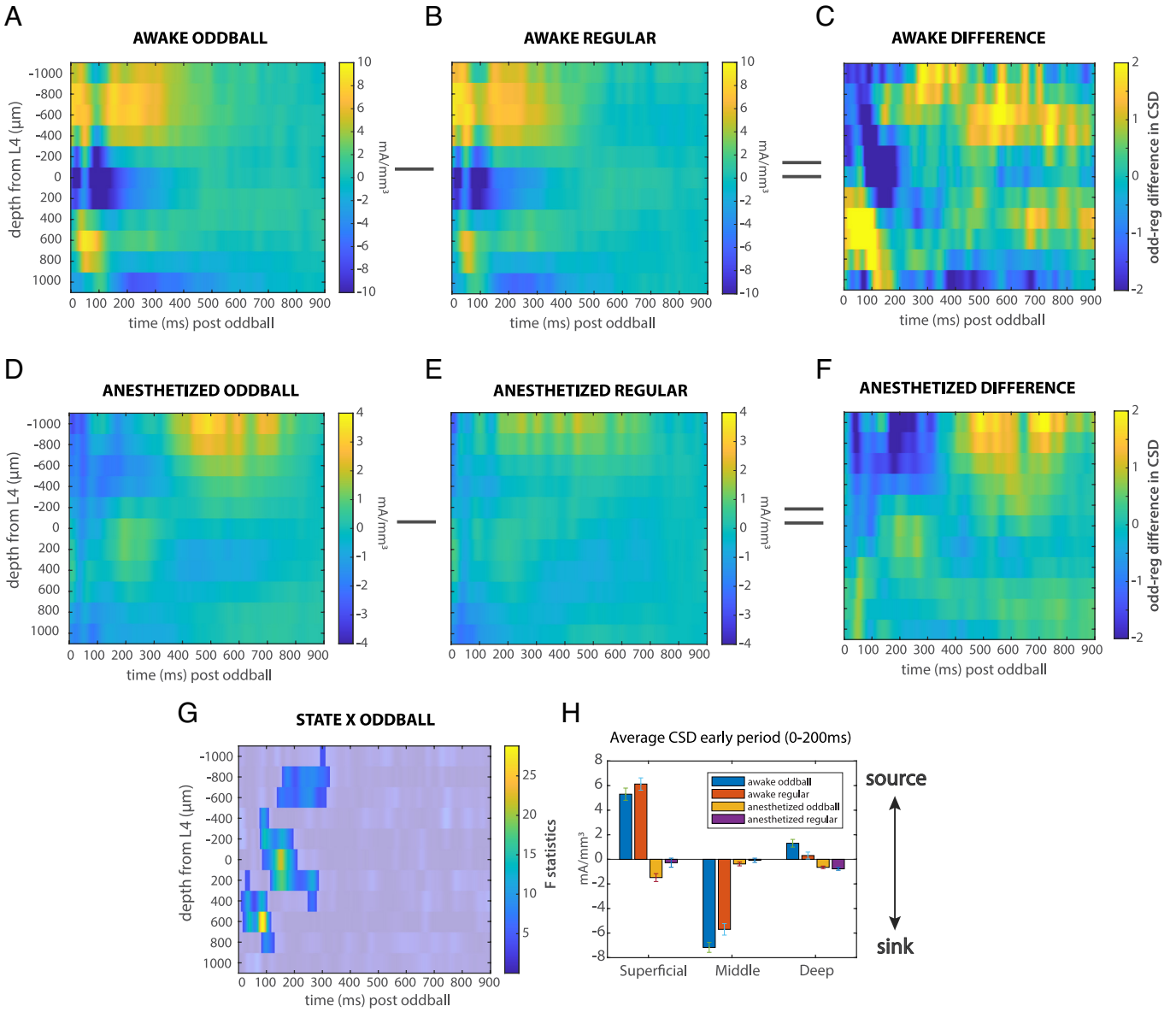

Fig. 4. Panels (*A*–*F*): Sensory region Tpt CSD responses during oddball (panel *A*) and regular trials (panel *B*) during awake state; CSD responses during oddball (panel *D*) and regular trials (panel *E*) during LOC. Zeros on the *x*-axis indicate the time of oddball presentation. Y-axes represent cortical depth (higher on the graph corresponds to closer to pia mater; negative numbers correspond to superficial layers, e.g., layers 2/3 and positive numbers correspond to deep layers, e.g., layers 5/6. The position of layer 4 is depth 0; see *Materials and Methods*). Difference in CSD between oddball trials vs. regular trials in Tpt during awake state (panel *C*) and during LOC (panel *F*); Panel (*G*): significant clusters of state-by-oddball interaction effects, FWE-corrected; Panel (*H*): CSD values for superficial vs. *Middle* vs. deep layers for early period (0 to 200 ms).

A = 0.0033 in Tpt, mean A = 0.0018 in FEF; mean per channel percent decrease in Tpt = 81.1%, mean per channel percent decrease in FEF = 79.9%; $P < 0.001$). Interestingly, in area Tpt, gamma coupling was stronger than beta (Fig. 5, rank sum test, $P < 0.05$). In area FEF, alpha/beta coupling was stronger than gamma (Fig. 5, rank sum test, $P < 0.05$).

The phase relationship between incoming spikes and the phase of an oscillation has been causally shown to modulate neuronal communication and behavioral responses (47, 48). What this prior work demonstrated is that the phase of incoming spikes may critically determine their impact on the local network. To investigate the effect of propofol on such phase specificity of spike-LFP phasic modulation, we examined the displacement parameters of the sinusoidal fits, which corresponds to the peak-to-trough phase specificity of the spike-field coupling. Propofol significantly shifted and disrupted this specificity in both frequency bands (Fig. 5, *Lower* subpanels). In alpha/beta band, spike-LFP phasic modulation had a mean displacement of 1.62 rad (peak to trough) in Tpt in awake state, compared to 1.26 rad (between peak to trough, but phase advanced ←) during LOC (rank sum test, $P < 0.05$), and 0.02 rad (around peak) in FEF, compared to −0.15 rad (around peak) during LOC (*ns*). In gamma band, LFP phase coupling with spiking has a mean displacement of 1.15 rad (peak to trough) in Tpt in awake state, compared to 0.71 (peak to trough, but phase advanced ←) rad during LOC ($P < 0.05$), and 1.00 rad (peak to trough) in FEF, compared to 0.35 (around peak, phase advanced ←) rad during LOC (rank sum test, $P < 0.05$). Of note, the distribution of FEF spike-alpha/beta coupling displacement was bimodal, unlike spike-LFP phasic modulation in other frequency/areas.

To test the effect of propofol on interareal spike-LFP phasic modulation, the same sinusoidal fitting procedure was done for all interareal channel pairs (Tpt phase–FEF MUA, and FEF phase–Tpt MUA, for both alpha/beta and gamma bands). Overall, the

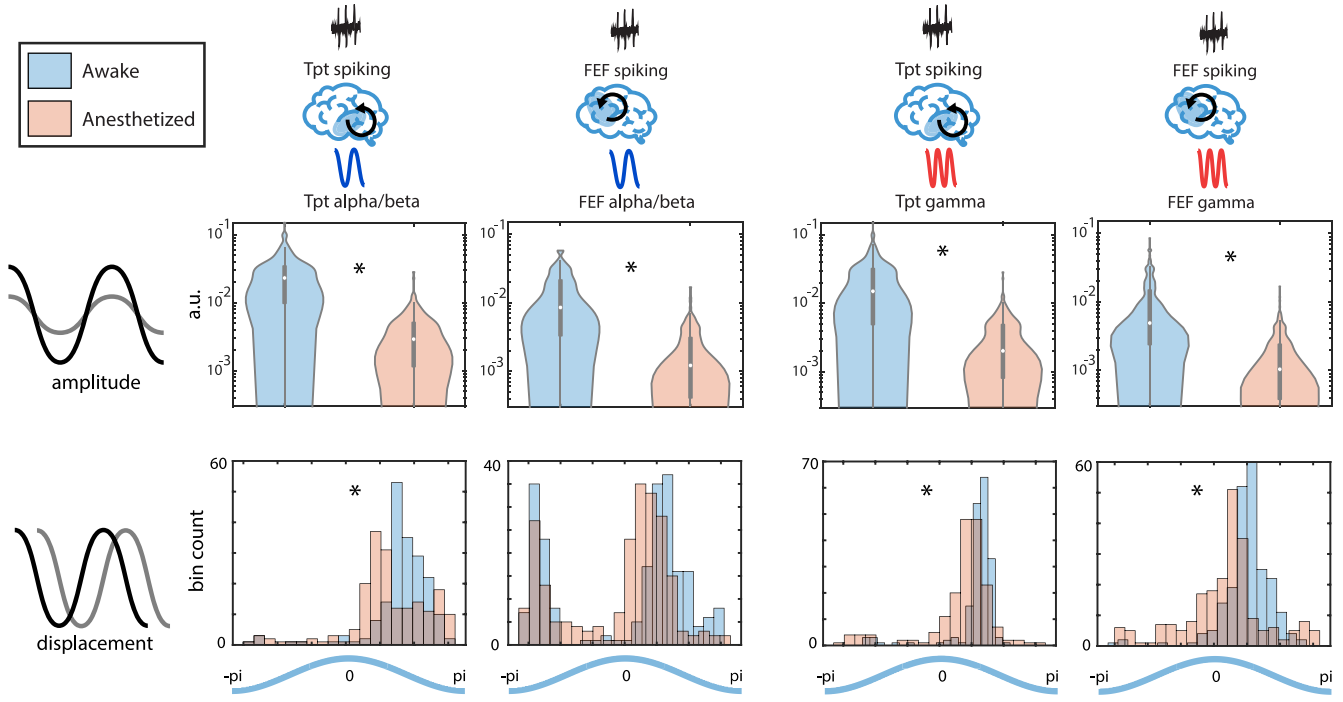

Fig. 5. Amplitude and displacement parameters of curve fits to within-area spiking-LFP coupling. N = 128 auditory-responsive Tpt channels, N = 99 auditory-responsive FEF channels. Asterisks (*) indicate significant differences between awake and unconscious states. Violin plot schematics: white dots indicate medians, shaded areas represent kernel density estimates, notches represent *Upper* and *Lower* quartiles, and whiskers indicate range.

interareal goodness-of-fit was lower than that of local (but still significant) sinusoidal fits in both frequency bands (alpha/beta: mean awake r^2 = 0.59 from Tpt MUA–FEF LFP phase fits, mean awake r^2 = 0.55 from FEF MUA–Tpt LFP phase fits; gamma: mean awake r^2 = 0.59 from Tpt MUA–FEF LFP phase fits, mean awake r^2 = 0.47 from FEF MUA–Tpt LFP phase fits). Consistently, the amplitudes of the sinusoidal fits were significantly decreased in both interareal directions and both frequency bands (Fig. 6, *Upper* subpanels, alpha/beta: mean A = 0.0022 for Tpt MUA by FEF LFP phase fits during awake state, mean A = 0.0014 during LOC, mean per channel percent decrease = 24.8%; mean A = 0.0013 for FEF MUA by Tpt LFP phase fits during awake state, mean A < 0.0001 during LOC, mean per channel percent decrease = 31.9%; gamma: mean A = 0.0016 from Tpt MUA by FEF LFP phase during awake state, mean A < 0.0001 during LOC, mean per channel percent decrease = 58.3%; mean A = 0.0010 from FEF MUA by Tpt LFP phase during awake state, mean A < 0.0001 during LOC, mean per channel percent decrease = 61.3%).

Sinusoidal fits of interareal LFP phase-spiking coupling also showed displacement shifts during LOC (Fig. 6, *Lower* subpanels). In alpha/beta band, Tpt LFP phase coupling with FEF MUA had a mean displacement of 0.50 rad (peak to trough) in awake state, compared to 0.03 rad (around peak, phase advanced ←) during LOC (rank sum test, $P < 0.05$). FEF LFP phase coupling with Tpt MUA had a mean displacement of 1.07 rad (peak to trough) in awake state, compared to 0.47 rad (peak to trough, phase advanced ←) during LOC (rank sum test, $P < 0.05$). In gamma band, Tpt LFP phase coupling with FEF MUA had a mean displacement of −0.30 rad (trough to peak) in awake state, compared to −0.21 rad (trough to peak, but phase delayed →) during LOC (rank sum test, $P < 0.05$); FEF LFP phase coupling with Tpt MUA had a mean displacement of 1.12 rad (peak to trough) in awake state, compared to 0.20 rad (peak to trough, but phase advanced) during LOC (rank sum test, $P < 0.05$).

Note that the same analysis was performed at a narrower bandwidth (15 to 20 Hz) for alpha/beta to reproduce the results to ensure that the wideband alpha/beta is capturing the modulatory effect of LFP phase (*SI Appendix*, Fig. S9).

Last, we analyzed whether these metrics of spike-LFP phasic modulation change in strength during oddball vs. regular trials (*SI Appendix*, Fig. S10). During the awake state, interareal phasic modulation between FEF and Tpt alpha/beta phase was significantly modulated by oddball status ($P < 0.05$). During the anesthetized state, only the interareal phasic modulation between Tpt spiking and FEF gamma phase was significantly modulated.

Discussion

Interruption of the Inhibitory Feedback Component of Predictive Routing in LFP, MUA, Single-Unit Spiking, and CSD. To test the predictive routing model and its role in conscious processing, we devised this study to include both feedforward (prediction error elicited by oddball trials) and feedback (prediction established by repeated regular trials) components, under awake state vs. propofol-mediated LOC. In line with recent reports (22, 49), we found striking differences in overall spiking rate during awake state vs. anesthetized state regardless of task condition (Fig. 1*A* and *SI Appendix*, Fig. S1).

Cortical feedforward information has been proposed to be carried by gamma and feedback by alpha/beta (11, 13, 50). The predictive routing model posits that alpha/beta band prepares the sensory cortex by inhibiting representations that are predicted (10). This was corroborated by our results which showed that in the awake state, in which gamma power was increased to local oddball trials and alpha/beta power was decreased compared to local regular trials and below spontaneous baseline activity. Many have argued that feedback processing is an integral information stream to support consciousness (25, 51). In line with the predictive routing model, the absence or degradation of feedback processing will disrupt predictive processing as well as the state of consciousness. Indeed, under propofol-mediated LOC, the inhibitory function

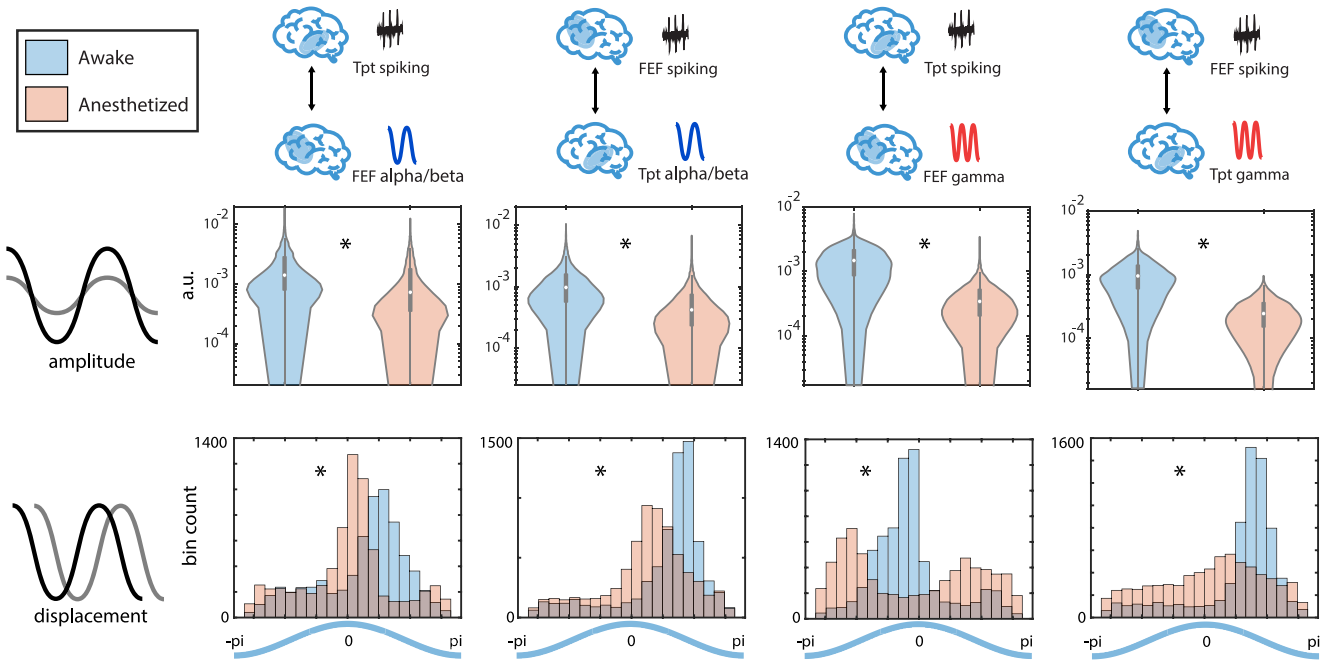

Fig. 6. Amplitude and displacement parameters of curve fits to interareal spiking-LFP coupling. N = 128 auditory-responsive Tpt channels, N = 99 auditory-responsive FEF channels. Asterisks (*) indicate significant differences between awake and unconscious states. Violin plot schematics: white dots indicate medians, shaded areas represent kernel density estimates, notches represent *Upper* and *Lower* quartiles, and whiskers indicate range.

of alpha/beta become diminished and/or eliminated, leading to disinhibition of oddballs in the sensory cortex. A similar reduction in alpha/beta power during auditory processing and increase in gamma power during propofol-mediated LOC was also recently reported in human intracranial recordings (52).

A competing hypothesis to consider is that oddball effects may be solely driven by neuronal adaptation. Indeed, neuronal adaptation causes decreased firing rate to repeated stimuli, and increased firing to an immediately presented novel stimulus due to release from adaptation. Further, neuronal adaptation also can be affected by anesthesia and conscious states (53). Nevertheless, our results of differential spiking to local oddball/global oddball and local oddball/global regular trials (Fig. 2*B*), as well as significant decoding of global oddball status at the population-level provide evidence that the oddball effects we report cannot be explained by neuronal adaptation (*SI Appendix*, Fig. S5). This is because local regular/global oddball and local regular/global regular trials have the same local pattern (e.g., AAAAA rare compared to AAAAA frequent), such that short-term neuronal adaptation should be equated. This suggests that there exist predictive processing mechanisms in the cortex beyond neuronal adaptation that require cortical feedback.

We consider top–down alpha/beta feedback to be largely inhibitory in nature because it is associated with predictions which tend to decrease activity. Gamma and spiking generally decrease with repeated and/or unpredicted stimuli, while alpha/beta increases. To note, there is a rich amount of literature regarding decreased alpha/beta as associated with top–down attention (54, 55), which is typically thought to be mediated via excitatory top–down feedback. The mechanisms by which top–down feedback becomes net excitatory (typically the case with attention) vs. net inhibitory (typically the case with prediction) remain unknown. Further studies should disentangle these elements by separately manipulating prediction vs. attention while measuring top–down feedback.

Also of note is the hierarchical nature of prediction error encoding. The hierarchical nature of predictive processing both in terms of cortical hierarchy and predictive complexity has been closely studied, including in humans. For example, Nourski et al. (37) used a similar paradigm to investigate the effect of LOC on predictive processing in human patients. As in our study, Nourski et al. found that LOC eliminated local oddball processing outside of the auditory cortex, and completely eliminated global oddball processing in both auditory and higher-order cortex. Consistent with this work, we find that local oddball processing was preserved (and prolonged) only in the auditory cortex under propofol-mediated LOC. In FEF, differential response to local oddball in MUA is eliminated. This hierarchical difference also suggests that predictive processing is not merely a result of neuronal adaptation, exhibited as decrease in firing rate due to local cellular mechanisms (56). For example, the strength of neuronal adaptation also shows hierarchical differences. FEF spiking adapts to near-baseline after a single auditory tone, whereas Tpt spiking slowly adapts over several tones (Fig. 2*A*). In addition, global oddballs are not encoded in mean firing rate across a population of neurons, but was decodable based on population spiking patterns in the higher-order cortex (*SI Appendix*, Fig. S5). In addition, global oddball trials that are also local oddball trials evoke significantly more spiking than global regular trials that are also local oddball trials (e.g., unpredicted vs. predicted AAAAB, Fig. 2*B*). Indeed, previous work has shown that global prediction error is a higher-level, complex, state-dependent computation (8, 57, 58), and studies have shown that global oddballs can be decoded by neuronal activity in PFC (39), implying an important role of frontal and prefrontal regions in predictive processing. This suggests that with no learning period, when the lower-order cortex detects an oddball within its processing time window (i.e., a non-repeating stimulus, or a local oddball), this information is fed forward, allowing the higher-order cortex to compute higher-level prediction error at a signal strength detectable at population average. If the lower-order cortex computation does not result in a prediction error, the higher-order cortex may only encode complex prediction error with a population pattern, perhaps unless this

pattern is learned/reinforced over time (59). This further corroborates with the idea that predictive processing is hierarchical and involves top–down feedback.

Moving beyond the scope of Nourski et al. (37), we observed a disruption of the feedback stream during LOC in LFP power, current source density, as well as disruption in spike-LFP phasic modulation. In LFP power, propofol-mediated LOC significantly reduced alpha/beta down-modulation during prediction, both in auditory cortex and in frontal cortex. Frontal cortex spiking to oddballs was eliminated during LOC. In area Tpt, there was a significant loss of spiking in the early period to oddballs during LOC. Loss of initial early peak is suggestive of decreased feedforward inputs from earlier sensory areas (60), likely reflecting the systemic GABAergic effect of propofol. Next, there was an enhanced and sustained oddball (prediction error) spiking response in sensory area Tpt. This delayed enhancement is in line with the hypothesis that inhibitory feedback from the higher cortex is disrupted. This disruption of the feedback stream allows the feedforward stream to become disinhibited. This is also exhibited in the prolonged enhancement of prediction error gamma power during LOC (compared to awake state, Fig. 3*A*). Note that while many previous studies have also identified a late component in awake oddball processing (9, 61) (as so did we) as a signature of consciousness, we consider this late component under anesthesia to be functionally distinct. Specifically, we hypothesize that the late component is a signature of disinhibited activity due to a lack of inhibitory feedback and the slowing of overall temporal dynamics in the system (e.g., enhanced slow wave implying increased time constants of neuronal activity). Similarly, the emergence of a greater superficial sink during prediction error vs. prediction also suggests the disinhibited feedforward process hypothesis. This greater superficial sink is well positioned near L3, which is the known output layer for feedforward projections (15).

Phasic Coupling of Beta/Gamma LFP and MUA within- and Interareas Is Disrupted by Propofol-Mediated LOC. Within-area spike-field coupling is often interpreted as the strength of local computation, often functionally relevant in domains such as attention (16, 31, 45). Interareal spike-field coupling, on the other hand, is interpreted as the strength of communication and information flow (31, 32). The disruption of local computation and interareal connectivity has been hypothesized to be a mechanism of anesthesia-mediated LOC (22, 62). In our analysis, we examined the amplitude and phasic shift of a sinusoidal fit from alpha/beta and gamma band phase onto multi-unit activity, both within-area and interareas.

Our results revealed that both alpha/beta and gamma band LFP phase strongly modulate both local and interareal multi-unit activity in the awake state. Under propofol-mediated LOC, this phasic modulation decreases, both within-area and interareas. This suggests that propofol disrupts local computation as well as interareal communication. The phase specificity of within-area spike timing to LFP oscillations has been argued to encourage efficient information encoding via summation of potentials (63, 64). In other words, there exists an optimal LFP phase to spiking activity peak that allows for maximal information encoding in the cortex (47, 48). This optimal phase to spiking activity peak is not achieved under propofol, suggesting a lag in communication between neural rhythms caused by this anesthetic.

Furthermore, our task modulation of spike-LFP phasic modulation analysis revealed that, during the awake state, phasic modulation between Tpt and FEF was significantly different during oddball trials vs. regular trials. During propofol-mediated LOC, only the interareal modulation in the gamma band was modulated by task. This suggests that the disinhibited spiking responses to oddball in Tpt can drive gamma in FEF, but the overall levels of spike-LFP phasic modulation between distant nodes are insufficient to drive conscious processing.

Implication on Theories of Consciousness: IIT vs. GNW? Recent ongoing debates between two leading theories of consciousness have called for empirical evidence (28). The authors list three diverging predictions from each theory. We address two of these predictions with our results below:

Prediction #1: *decoding area of conscious content*. IIT posits that posterior hot zones are primarily responsible for conscious content. GNW theory posits that frontal areas (and their connections) are necessary for conscious content. During propofol-mediated LOC, we observed enhanced late spiking, gamma power, and superficial layer current sinks to unpredictable vs. predictable stimuli in Tpt. Our results show that posterior region activity alone is insufficient for conscious perception. Propofol-mediated LOC was marked by the elimination of prefrontal differential spiking to oddballs. Furthermore, our population-based decoding analysis showed that while global oddball status was decodable under awake state in PFC and FEF, this decoding was eliminated under LOC. This is consistent with many studies that investigated the role of frontal and prefrontal areas, particularly PFC, in conscious perception (35, 42, 61, 65–67). Our results therefore suggest an important role for prefrontal cortex activation, in addition to sensory cortex activation, for conscious perception consistent with GNW theory.

Prediction #2: *interareal connectivity during conscious perception*. IIT posits that conscious perception is marked by short-range interactions/connectivity in posterior regions. GNW theory posits that conscious perception is marked by long-range feedforward/feedback connectivity between lower- and higher-order cortical areas and that feedforward connectivity alone is insufficient to drive conscious processing. During propofol-mediated LOC, gamma spike-LFP phasic modulation between Tpt and FEF increased during oddballs compared to regular tones, an increase in feedforward influence. However, overall levels of beta/gamma spike-LFP phasic modulation both within and between areas were significantly lower when comparing LOC vs. wakefulness. The lack of conscious processing despite residual feedforward signaling supports the GNW model, whereby overall levels of phasic interareal interaction were incapable of providing sufficient communication to enable network "ignition." At the same time, our finding of an overall strong reduction in spike-LFP phasic modulation in the sensory cortex is consistent with IIT. Thus, we interpret our results to provide some support for aspects of both theories for Prediction #2.

In sum, in line with the predictive routing model, alpha/beta oscillations in the awake state serve to inhibit the processing of predictable stimuli. Propofol-mediated LOC eliminates alpha/beta modulation in the sensory cortex and alpha/beta phasic modulation between sensory and frontal areas. As a result, we propose, oddball stimuli cause enhanced gamma power, late period spiking, and superficial layer sinks in the sensory cortex. Therefore, somewhat paradoxically, the auditory cortex is in a disinhibited state during propofol-mediated LOC when processing oddballs. However, despite these enhanced feedforward responses in the auditory cortex, there is a loss of an oddball response in the higher-order cortex. The inability of the sensory cortex to effectively drive higher-order cortex may be the result of a loss of within- and interareal spike-field coupling in the alpha/beta and gamma frequencies. In addition, these results provide empirical

evidence for the IIT vs. GNW debate: Activation of the posterior sensory cortex is insufficient for conscious processing. Instead, conscious processing is promoted by activation of both sensory and frontal cortices to an oddball, together with intact within- and interarea oscillatory dynamics at both alpha/beta and gamma frequencies.

Materials and Methods

We recorded spiking and LFP activity in auditory and frontal areas with Utah arrays and laminar probes in 2 macaque monkeys (*Macaca mulatta*) during a passive auditory local/global oddball task (8). We analyzed spiking activity (including mean firing and population decoding analysis), LFP, CSD, and functional connectivity in response to the experimental stimuli. All surgical and animal care procedures were approved by the Massachusetts Institute of Technology's (MIT) Committee on Animal Care and were conducted in accordance with the guidelines of the NIH and MIT's Department of Comparative Medicine. A detailed description of the study methodology is provided in *SI Appendix*.

Data, Materials, and Software Availability. Data have been deposited in Figshare (https://doi.org/10.6084/m9.figshare.26980630) (68). All processed data are available in manuscript and/or *SI Appendix*.

ACKNOWLEDGMENTS. We would like to thank Charles Shvartsman for help with initial analyses of this dataset. This work was supported by National Institute of Mental Health R00MH116100, National Institute of General Medical Sciences P01GM118269, National Institute of Mental Health R01MH115592, National Institute of Mental Health 1R01MH131715-01, the JPB Foundation, The Picower Institute for Learning and Memory, The Simons Foundation for the Social Brain, George J. Elbaum (MIT'59, SM'63, PhD'67), Mimi Jensen, Diane B. Greene (MIT, SM'78), Mendel Rosenblum, Lou Paglia (MIT' 79), Cathy Paglia and Bill Swanson, annual donors to the MIT-Harvard BASCIC Fund; National Institute of Neurological Disorders and Stroke R01 NS123120-03, and Vanderbilt University startup funds.

Author affiliations: [a]Department of Psychology, Vanderbilt University, Nashville, TN 37235; [b]The Picower Institute for Learning and Memory and Department of Brain and Cognitive Sciences, Massachusetts Institute of Technology, Cambridge, MA 02139; [c]Division of Psychology, Department of Clinical Neuroscience, Karolinska Institute, Stockholm 171 77, Sweden; [d]The Department of Anesthesia, Critical Care and Pain Medicine, Massachusetts General Hospital/Harvard Medical School, Boston, MA 02114; [e]The Institute for Medical Engineering and Science, Massachusetts Institute of Technology, Cambridge, MA 02139; and [f]Vanderbilt Brain Institute, Vanderbilt University, Nashville, TN 37240

Author contributions: E.N.B., E.K.M., and A.M.B. designed research; J.A.D., M.L., M.M., and A.M.B. performed research; Y.S.X. and A.M.B. analyzed data; E.N.B., E.K.M., and A.M.B. supervised research; Y.S.X. and A.M.B. wrote the paper; and all authors edited the manuscript.

Competing interest statement: E.N.B. holds patents on anesthetic state monitoring and control. E.N.B. holds founding interest in PASCALL, a start-up developing physiological monitoring systems; receives royalties from intellectual property through Massachusetts General Hospital licensed to Masimo. The interests of E.N.B. were reviewed and are managed by Massachusetts General Hospital and Mass General Brigham in accordance with their conflict of interest policies.

1. H. Helmholtz, *Handbuch der Physiologischen Optik* [in German], J. P. C. Southall, Ed. (Leopold Voss Verlag, Hamburg, Leipzig, 1860).
2. A. M. Bastos *et al.*, Canonical microcircuits for predictive coding. *Neuron* **76**, 695–711 (2012).
3. K. Friston, S. Kiebel, Predictive coding under the free-energy principle. *Philos. Trans. R Soc. B Biol. Sci.* **364**, 1211–1221 (2009).
4. R. P. N. Rao, D. H. Ballard, Predictive coding in the visual cortex: A functional interpretation of some extra-classical receptive-field effects. *Nat. Neurosci.* **2**, 79–87 (1999).
5. A. H. Bell, C. Summerfield, E. L. Morin, N. J. Malecek, L. G. Ungerleider, Encoding of stimulus probability in macaque inferior temporal cortex. *Curr. Biol.* **26**, 2280–2290 (2016).
6. K. Rauss, S. Schwartz, G. Pourtois, Top-down effects on early visual processing in humans: A predictive coding framework. *Neurosci. Biobehav. Rev.* **35**, 1237–1253 (2011).
7. S. Kumar *et al.*, Predictive coding and pitch processing in the auditory cortex. *J. Cogn. Neurosci.* **23**, 3084–3094 (2011).
8. T. A. Bekinschtein *et al.*, Neural signature of the conscious processing of auditory regularities. *Proc. Natl. Acad. Sci. U.S.A.* **106**, 1672–1677 (2009).
9. Z. C. Chao, K. Takaura, L. Wang, N. Fujii, S. Dehaene, Large-scale cortical networks for hierarchical prediction and prediction error in the primate brain. *Neuron* **100**, 1252–1266 (2018).
10. A. M. Bastos, M. Lundqvist, A. S. Waite, N. Kopell, E. K. Miller, Layer and rhythm specificity for predictive routing. *Proc. Natl. Acad. Sci. U.S.A.* **117**, 31459–31469 (2020).
11. A. M. Bastos *et al.*, Visual areas exert feedforward and feedback influences through distinct frequency channels. *Neuron* **85**, 390–401 (2015).
12. G. Michalareas *et al.*, Alpha-beta and gamma rhythms subserve feedback and feedforward influences among human visual cortical areas. *Neuron* **89**, 384–397 (2016).
13. T. Van Kerkoerle *et al.*, Alpha and gamma oscillations characterize feedback and feedforward processing in monkey visual cortex. *Proc. Natl. Acad. Sci. U.S.A.* **111**, 14332–14341 (2014).
14. D. J. Felleman, D. C. Van Essen, Distributed hierarchical processing in the primate cerebral cortex. *Cereb. Cortex* **1**, 1–47 (1991).
15. N. T. Markov *et al.*, Anatomy of hierarchy: Feedforward and feedback pathways in macaque visual cortex. *J. Comp. Neurol.* **522**, 225–259 (2014).
16. E. A. Buffalo, P. Fries, R. Landman, T. J. Buschman, R. Desimone, Laminar differences in gamma and alpha coherence in the ventral stream. *Proc. Natl. Acad. Sci. U.S.A.* **108**, 11262 (2011).
17. A. M. Bastos, R. Loonis, S. Kornblith, M. Lundqvist, E. K. Miller, Laminar recordings in frontal cortex suggest distinct layers for maintenance and control of working memory. *Proc. Natl. Acad. Sci. U.S.A.* **115**, 1117–1122 (2018).
18. D. Mendoza-Halliday *et al.*, A ubiquitous spectrolaminar motif of local field potential power across the primate cortex. *Nat. Neurosci.* **27**, 547–560 (2024).
19. A. Maier, C. J. Aura, D. A. Leopold, Infragranular sources of sustained local field potential responses in macaque primary visual cortex. *J. Neurosci.* **31**, 1971–1980 (2011).
20. S. Haegens *et al.*, Laminar profile and physiology of the α rhythm in primary visual, auditory, and somatosensory regions of neocortex. *J. Neurosci.* **35**, 14341–14352 (2015).
21. R. Sanchez-Todo *et al.*, A physical neural mass model framework for the analysis of oscillatory generators from laminar electrophysiological recordings. *Neuroimage* **270**, 119938 (2023).
22. A. M. Bastos *et al.*, Neural effects of propofol-induced unconsciousness and its reversal using thalamic stimulation. *Elife* **10**, e60824 (2021), 10.7554/eLife.60824.
23. E. N. Brown, R. Lydic, N. D. Schiff, General anesthesia, sleep, and coma. *N. Engl. J. Med.* **363**, 2638–2650 (2010).
24. M. J. Redinbaugh *et al.*, Thalamus modulates consciousness via layer-specific control of cortex. *Neuron* **106**, 66–75 (2020).
25. S. Dehaene, M. Kerszberg, J. P. Changeux, A neuronal model of a global workspace in effortful cognitive tasks. *Proc. Natl. Acad. Sci. U.S.A* **95**, 14529–14534 (1998).
26. G. Tononi, Consciousness as integrated information: A provisional manifesto. *Biol. Bull.* **215**, 216–242 (2008).
27. C. Koch, M. Massimini, M. Boly, G. Tononi, Posterior and anterior cortex–Where is the difference that makes the difference? *Nat. Rev. Neurosci.* **17**, 666–666 (2016).
28. L. Melloni *et al.*, An adversarial collaboration protocol for testing contrasting predictions of global neuronal workspace and integrated information theory. *PLoS One* **18**, e0268577 (2023).
29. Z. W. Davis, N. M. Dotson, T. P. Franken, L. Muller, J. H. Reynolds, Spike-phase coupling patterns reveal laminar identity in primate cortex. *Elife* **12**, e84512 (2023).
30. P. Fries, J. H. Reynolds, A. E. Rorie, R. Desimone, Modulation of oscillatory neuronal synchronization by selective visual attention. *Science* **291**, 1560–1563 (2001).
31. I. C. Fiebelkorn, S. Kastner, Spike timing in the attention network predicts behavioral outcome prior to target selection. *Neuron* **109**, 177–188 (2021).
32. G. G. Gregoriou, S. J. Gotts, H. Zhou, R. Desimone, High-frequency, long-range coupling between prefrontal and visual cortex during attention. *Science* **324**, 1207–1210 (2009).
33. L. Uhrig, S. Dehaene, B. Jarraya, A hierarchy of responses to auditory regularities in the macaque brain. *J. Neurosci.* **34**, 1127–1132 (2014).
34. I. El Karoui *et al.*, Event-related potential, time-frequency, and functional connectivity facets of local and global auditory novelty processing: An intracranial study in humans. *Cerebr. Cortex* **25**, 4203–4212 (2015).
35. L. Uhrig, D. Janssen, S. Dehaene, B. Jarraya, Cerebral responses to local and global auditory novelty under general anesthesia. *Neuroimage* **141**, 326–340 (2016).
36. J. H. Kaas, T. A. Hackett, Subdivisions of auditory cortex and processing streams in primates. *Proc. Natl. Acad. Sci. U.S.A.* **97**, 11793–11799 (2000).
37. K. V. Nourski *et al.*, Auditory predictive coding across awareness states under anesthesia: An intracranial electrophysiology study. *J. Neurosci.* **38**, 8441–8452 (2018).
38. C. Wacongne *et al.*, Evidence for a hierarchy of predictions and prediction errors in human cortex. *Proc. Natl. Acad. Sci. U.S.A.* **108**, 20754–20759 (2011).
39. M. E. Bellet *et al.*, Spontaneously emerging internal models of visual sequences combine abstract and event-specific information in the prefrontal cortex. *Cell Rep.* **43**, 113952 (2024).
40. L. H. Arnal, V. Wyart, A.-L. Giraud, Transitions in neural oscillations reflect prediction errors generated in audiovisual speech. *Nat. Neurosci.* **14**, 797–801 (2011).
41. A. Todorovic, F. van Ede, E. Maris, F. P. de Lange, Prior expectation mediates neural adaptation to repeated sounds in the auditory cortex: An MEG study. *J. Neurosci.* **31**, 9118–9123 (2011).
42. A. Dwarakanath *et al.*, Bistability of prefrontal states gates access to consciousness. *Neuron* **111**, 1666–1683 (2023).
43. U. Mitzdorf, Current source-density method and application in cat cerebral cortex: Investigation of evoked potentials and EEG phenomena. *Physiol. Rev.* **65**, 37–100 (1985).
44. D. C. Godlove, A. Maier, G. F. Woodman, J. D. Schall, Microcircuitry of agranular frontal cortex: Testing the generality of the canonical cortical microcircuit. *J. Neurosci.* **34**, 5355–5369 (2014).
45. T. J. Buschman, E. K. Miller, Top-down versus bottom-up control of attention in the prefrontal and posterior parietal cortices. *Science* **315**, 1860–1862 (2007).
46. J. Ni *et al.*, Gamma-rhythmic gain modulation. *Neuron* **92**, 240–251 (2016).
47. E. Drebitz, L.-P. Rausch, A. K. Kreiter, Neuronal information processing causally depends on gamma phase synchrony. Research Square [Preprint] (2023). https://doi.org/10.21203/rs.3.rs-3011004/v1 (Accessed 19 August 2023).
48. J. H. Siegle, D. L. Pritchett, C. I. Moore, Gamma-range synchronization of fast-spiking interneurons can enhance detection of tactile stimuli. *Nat. Neurosci.* **17**, 1371–1379 (2014).
49. J. M. Tauber *et al.*, Propofol-mediated unconsciousness disrupts progression of sensory signals through the cortical hierarchy. *J. Cogn. Neurosci.* **36**, 394–413 (2024).
50. W. Turner, T. Blom, H. Hogendoorn, Visual information is predictively encoded in occipital alpha/low-beta oscillations. *J. Neurosci.* **43**, 5537–5545 (2023).

51. C. P. Casey *et al.*, Dynamic causal modelling of auditory surprise during disconnected consciousness: The role of feedback connectivity. *Neuroimage* **263**, 119657 (2022).
52. A. J. Krom *et al.*, Anesthesia-induced loss of consciousness disrupts auditory responses beyond primary cortex. *Proc. Natl. Acad. Sci. U.S.A.* **117**, 11770–11780 (2020).
53. M. A. Castro-Alamancos, Absence of rapid sensory adaptation in neocortex during information processing states. *Neuron* **41**, 455–464 (2004).
54. S. Haegens, B. F. Händel, O. Jensen, Top-down controlled alpha band activity in somatosensory areas determines behavioral performance in a discrimination task. *J. Neurosci.* **31**, 5197–5204 (2011).
55. O. Jensen, A. Mazaheri, Shaping functional architecture by oscillatory alpha activity: Gating by inhibition. *Front. Hum. Neurosci.* **4**, 186 (2010).
56. D. Pérez-González, M. S. Malmierca, Adaptation in the auditory system: An overview. *Front. Integr. Neurosci.* **8**, 19 (2014).
57. M. Strauss *et al.*, Disruption of hierarchical predictive coding during sleep. *Proc. Natl. Acad. Sci. U.S.A.* **112**, E1353–E1362 (2015).
58. T. Teichert, H. Jedema, Z. Shen, K. Gurnsey, Mismatch responses mediated by adaptation and deviance detection have complementary functional profiles that point to different auditory short-term memory systems. bioRxiv [Preprint] (2019). https://doi.org/10.1101/2019.12.18.881821 (Accessed 27 May 2021).
59. K. Gabhart, Y. S. Xiong, A. Bastos, Where are global oddballs? A predictive routing theory. PsyArxiv [Preprint] (2023). https://doi.org/10.31234/osf.io/7sz3w (Accessed 6 August 2024).
60. M. W. Self, R. N. Kooijmans, H. Supèr, V. A. Lamme, P. R. Roelfsema, Different glutamate receptors convey feedforward and recurrent processing in macaque V1. *Proc. Natl. Acad. Sci. U.S.A.* **109**, 11031–11036 (2012).
61. J. Bellet *et al.*, Decoding rapidly presented visual stimuli from prefrontal ensembles without report nor post-perceptual processing. *Neurosci. Conscious.* 2022, niac005 (2022).
62. M. Boly *et al.*, Connectivity changes underlying spectral EEG changes during propofol-induced loss of consciousness. *J. Neurosci.* **32**, 7082–7090 (2012).
63. T. Womelsdorf *et al.*, Modulation of neuronal interactions through neuronal synchronization. *Science* **316**, 1609–1612 (2007).
64. A. Zandvakili, A. Kohn, Coordinated neuronal activity enhances corticocortical communication. *Neuron* **87**, 827–839 (2015).
65. T. I. Panagiotaropoulos, G. Deco, V. Kapoor, N. K. Logothetis, Neuronal discharges and gamma oscillations explicitly reflect visual consciousness in the lateral prefrontal cortex. *Neuron* **74**, 924–935 (2012).
66. V. Kapoor, M. Besserve, N. K. Logothetis, T. I. Panagiotaropoulos, Parallel and functionally segregated processing of task phase and conscious content in the prefrontal cortex. *Commun. Biol.* **1**, 215 (2018).
67. V. Kapoor *et al.*, Decoding internally generated transitions of conscious contents in the prefrontal cortex without subjective reports. *Nat. Commun.* **13**, 1535 (2022).
68. Y. Xiong, Data from "Propofol-mediated loss of consciousness disrupts predictive routing and local field phase modulation of neural activity." Figshare. https://doi.org/10.6084/m9.figshare.26980630.v1. Deposited 19 September 2024.